

Phase Correction in Microwave Fourier Transform Spectroscopy

N. Heineking and H. Dreizler

Institut für Physikalische Chemie, Universität Kiel, Olshausenstraße 40–60, D-2300 Kiel 1

Z. Naturforsch. **44a**, 573–576 (1989); received March 17, 1989

We report on our experience with the adaptation of phase correction techniques to microwave Fourier transform spectroscopy. The performance of this yet uncommon technique is based on theoretical considerations and compared to other methods.

Introduction

A general shortcoming of Fourier transform (FT) spectroscopy is the mixture of absorption and dispersion features in the complex Fourier transform spectrum. There are two means to overcome this disadvantage:

One possibility is to calculate the phase-independent power spectrum. This technique is used by most microwave Fourier transform (MWFT) spectroscopists. It is very fast but has the disadvantage of more severe line shape distortions [1]. These are essentially entailed by including the squared dispersion spectrum, which is, for the line shapes usually encountered, more broadly distributed in the frequency domain. Such distortions have led us to prefer fitting procedures, applied to the time domain data to obtain accurate line frequencies [2]. The disadvantage of the fit methods is that they may take more time than the original measurement did.

A second possibility is the so-called phase correction, which is commonly used in FT-nuclear magnetic resonance (FTNMR) and FT-infrared (FTIR) spectroscopy. With the assumption of a linear dependence of the degree of mixing of absorption and dispersion with frequency (or wavenumber in FTIR), the absorption spectrum is evaluated from the complex Fourier coefficients. The constant and proportional phase correction parameters (see (4)) are chosen so as to give symmetric and positive line shapes.

In the present work, we have tried to adopt the phase correction technique to MWFT spectroscopy and to calculate the absorption spectrum from the Fourier coefficients. Of course, the equations are essentially analogous to those used in the existing phase correction techniques [3].

Reprint requests to Prof. Dr. H. Dreizler, Institut für Physikalische Chemie der Christian-Albrechts-Universität zu Kiel, Ludewig-Meyn-Str. 8, D-2300 Kiel.

Theory

FT spectroscopy deals with molecular signals which start at a definite origin and extend either in both negative and positive directions, or in only one direction of the one-dimensional signal space (path difference in FTIR, time in FTNMR and MWFT). However, both the exact position of this origin and the exact signal phase at this origin may be unknown.

In MWFT spectroscopy, the transient emission signal may roughly be regarded as beginning when the short, intense polarizing microwave pulse is switched off, with the inverted phase as the polarizing wave. Afterwards one has to wait several hundred nanoseconds before data acquisition is feasible. For a particular spectrometer, this delay, d , can be controlled fairly accurately. What is not known, however, is the absolute phase of the transient emission, φ_0 , at the time the polarizing pulse is switched off. The relationship between the signal phases at the beginning of data acquisition, φ_1 (l labelling each line), and the line centre frequencies, ω_1 , is approximated by

$$\varphi_1 = \varphi_0 + \omega_1 d \quad (1)$$

with φ_0 and the accurate value of d unknown. However, we can estimate d , and can calculate the φ_1 's from the Fourier coefficients with the relation $\varphi_1 = -\arctan(b/a)$; a and b are the real and imaginary coefficient, respectively, at the approximate ω_1 's. Thus, for every line contained in the spectrum, we get one pair of data φ_1 and ω_1 . Therefore we can at least calculate φ_0 with our estimate for d .

In the following section, we calculate the effects of phase correction assuming a continuously sampled, Doppler-free, complex time-domain signal. This allows the most convenient mathematical treatment. In practice, one has to deal with Doppler broadened signals, which are discretely sampled and normally form a real data set, the imaginary part being set to

0932-0784 / 89 / 0600-0573 \$ 01.30/0. – Please order a reprint rather than making your own copy.



Dieses Werk wurde im Jahr 2013 vom Verlag Zeitschrift für Naturforschung in Zusammenarbeit mit der Max-Planck-Gesellschaft zur Förderung der Wissenschaften e.V. digitalisiert und unter folgender Lizenz veröffentlicht: Creative Commons Namensnennung-Keine Bearbeitung 3.0 Deutschland Lizenz.

Zum 01.01.2015 ist eine Anpassung der Lizenzbedingungen (Entfall der Creative Commons Lizenzbedingung „Keine Bearbeitung“) beabsichtigt, um eine Nachnutzung auch im Rahmen zukünftiger wissenschaftlicher Nutzungsformen zu ermöglichen.

This work has been digitalized and published in 2013 by Verlag Zeitschrift für Naturforschung in cooperation with the Max Planck Society for the Advancement of Science under a Creative Commons Attribution-NoDerivs 3.0 Germany License.

On 01.01.2015 it is planned to change the License Conditions (the removal of the Creative Commons License condition "no derivative works"). This is to allow reuse in the area of future scientific usage.

zeroes. However, the simplifications do not influence the conclusions to be drawn.

A pressure-broadened emission signal is in the time domain expressed by (A amplitude factor, T relaxation time)

$$X(t) = A \cdot \exp(-t/T) \cdot \exp(i\omega_1 t) \cdot \exp(i\phi_1) \quad (2)$$

with the complex Fourier transform

$$\begin{aligned} C(\omega) &= 1/2\pi \int X(t) \cdot \exp(-i\omega t) dt \\ &= A \cdot T \cdot \{1 + [(\omega - \omega_1)T]^2\}^{-1/2} \\ &\quad \cdot \exp\{-i \cdot \arctan[(\omega - \omega_1)T]\} \cdot \exp(i\phi_1). \end{aligned} \quad (3)$$

The phase correction is carried out (corrected quantities are primed) by multiplying this expression with $\exp[-i(\phi_c + \omega d_c)]$ (ϕ_c = estimate of ϕ_0 , d_c = estimate of d):

$$\begin{aligned} C'(\omega) &= A \cdot T \cdot \{1 + [(\omega - \omega_1)T]^2\}^{-1/2} \\ &\quad \cdot \exp\{-i \cdot \arctan[(\omega - \omega_1)T]\} \\ &\quad \cdot \exp[i(\phi_0 - \phi_c + \omega_1 d - \omega d_c)] \end{aligned} \quad (4)$$

or

$$\begin{aligned} a'(\omega) &= \text{Re}[C'(\omega)] = A \cdot T \cdot \{1 + [(\omega - \omega_1)T]^2\}^{-1} \\ &\quad \cdot \cos\{\arctan[(\omega - \omega_1)T] + (\phi_c - \phi_0) + \omega d_c - \omega_1 d\} \end{aligned} \quad (4a)$$

and

$$\begin{aligned} b'(\omega) &= -\text{Im}[C'(\omega)] = A \cdot T \cdot \{1 + [(\omega - \omega_1)T]^2\}^{-1} \\ &\quad \cdot \sin\{\arctan[(\omega - \omega_1)T] + (\phi_c - \phi_0) + \omega d_c - \omega_1 d\}. \end{aligned} \quad (4b)$$

Expressed as a function of $\Delta\omega = \omega - \omega_1$, the former reads (if, and only if, $\phi_c = \phi_0$ and $d_c = d$):

$$\begin{aligned} a'(\Delta\omega) &= A \cdot T \cdot [1 + (\Delta\omega T)^2]^{-1} \\ &\quad \cdot (\cos \Delta\omega d - \Delta\omega T \cdot \sin \Delta\omega d). \end{aligned} \quad (5)$$

If d would equal zero (which is impossible in MWFT), this would describe the common absorption line shape. Even if d is finite, the last term in brackets equals unity for $\Delta\omega = 0$ but will become negative for larger $\Delta\omega$ (d is always positive), so that the phase corrected absorption spectrum cannot be entirely positive (see Figure 1). However, the right-hand side of (5) is independent of the sign of $\Delta\omega$, so that the line shape remains symmetric for all values of d . In fact, both ϕ_c and d_c have to be adjusted using this criterion of symmetry. This is done by displaying the once corrected absorption spectrum and judging the line shapes: different line shapes for the various spectral lines indicate

an inaccurate choice of d_c , whereas equal, but non-symmetric line shapes are due to a faulty ϕ_c . In the case of narrow multiplets, the lines overlap to give non-symmetric features. In unfavourable cases, ambiguities may result. However, if there are at least two isolated lines sufficiently far apart, the phase correction can be carried out without introducing too large an error.

As a further result of (5), the lines appear narrower in the phase corrected spectrum than they would do in the normal absorption spectrum:

$$a(\Delta\omega_{1/2} = 1/T) = A \cdot T \cdot (1/2),$$

whereas (6)

$$a'(\Delta\omega_{1/2} = 1/T) = 1/2 \cdot A \cdot T \cdot [\cos(d/T) - \sin(d/T)],$$

where the term in square brackets is slightly less than unity (except for extreme values of d/T). However, in the immediate proximity of the peak position, the trigonometric terms may be expanded:

$$\cos(\Delta\omega d) \cong 1 - 1/2 \cdot (\Delta\omega d)^2 \quad \text{and} \quad \sin(\Delta\omega d) \cong \Delta\omega d. \quad (7)$$

If $\Delta\omega = 1/(T+d) \ll 1/d$, the spectral amplitude is thus approximated by

$$\begin{aligned} a'(\Delta\omega = 1/(T+d)) &= A \cdot T \cdot \frac{1 - \Delta\omega^2 (1/2 \cdot d^2 + Td)}{1 + \Delta\omega^2 T^2} \\ &= A \cdot T \cdot \frac{T^2 + 2Td + d^2 - 1/2 \cdot d^2 - Td}{T^2 + 2Td + d^2 + T^2} \\ &= 1/2 \cdot A \cdot T. \end{aligned} \quad (8)$$

This is just a modified definition of the half width at half maximum (HWHM). The normal HWHM in an absorption spectrum (and also in a power spectrum) is $\Delta\omega_{1/2} = 1/T$, instead of $1/(T+d) < 1/T$ in the phase corrected absorption spectrum. However, this apparent increase in resolution is paid for with the lower signal intensity due to the dephasing during the delay d : Let t' count the time from the beginning of data acquisition, and let t count the time from the beginning of emission. Then (2) may be rewritten

$$X(t') = \exp(-d/T) \cdot X(t) \cdot \exp(i\omega_1 d). \quad (2')$$

For $d \ll T$, the expansion of the first term yields

$$X(t') = (1 - d/T) \cdot X(t) \cdot \exp(i\omega_1 d). \quad (2'')$$

The damping factor of $(1 - d/T)$ is just the reciprocal of the line narrowing factor given above.

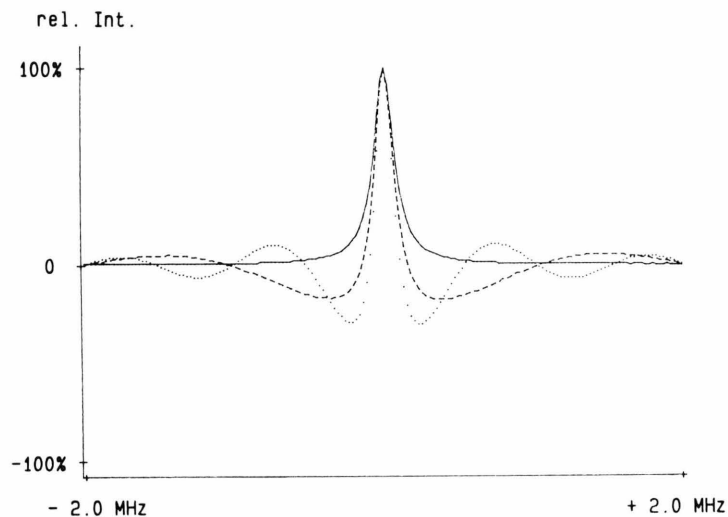


Fig. 1.

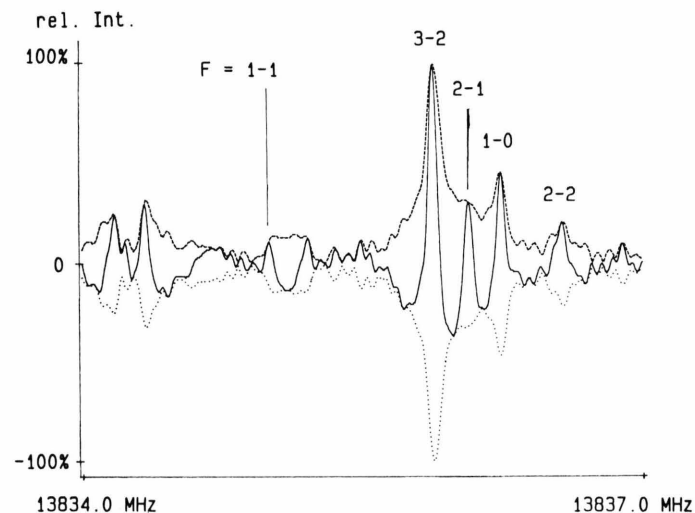


Fig. 3.

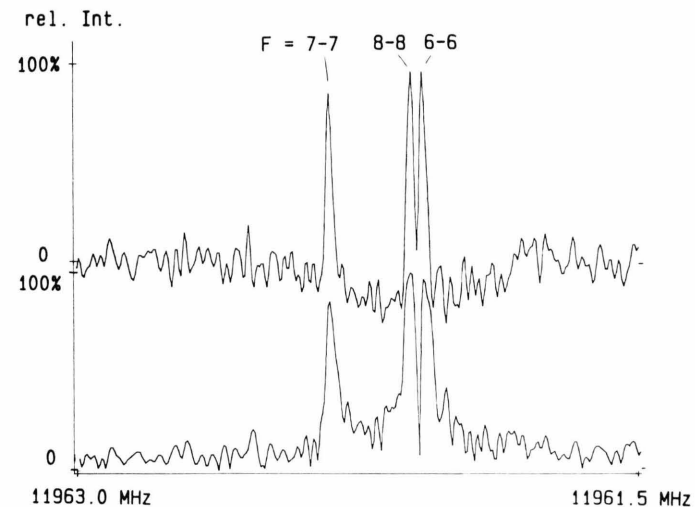


Fig. 2.

Fig. 1. The phase corrected absorption spectrum of a calculated Lorentzian line ($T=2\text{ }\mu\text{s}$) is displayed using different delays to show the influence on the line shape. – Solid line: $d=0$; dashed: $d=500\text{ ns}=T/4$; dotted: $d=1000\text{ ns}=T/2$.

Fig. 2. 1.5-MHz-range out of the rotational spectrum of pyridine-N-oxide, showing the transition $J, K_-, K_+=7, 2, 5-7, 2, 6$ split into three hyperfine components. F quantum numbers given. Cell temperature -30°C , pressure 0.1 Pa, data acquisition interval $50\text{ }\mu\text{s}$, FFT-length 4096 points. – Upper trace: phase corrected absorption spectrum ($d_c=1600\text{ ns}$); lower trace: amplitude spectrum.

Fig. 3. 3-MHz-range out of the rotational spectrum of 2-fluoroacetamide, $\text{FCH}_2\text{CONH}_2$, showing the rotational transition $J, K_-, K_+=2, 0, 2-1, 0, 1$. Acquisition interval $20\text{ }\mu\text{s}$, temperature -20°C , pressure 0.1 Pa, FFT-length 4096 points, delay $1.6\text{ }\mu\text{s}$. F quantum numbers are given. – Solid trace: phase corrected absorption spectrum; dashed/dotted trace: positive/negative root of power spectrum.

Another aspect is the influence on the signal-to-noise ratio. To judge this, we consider a series of, say, M individual recordings under identical conditions, each decay separately Fourier transformed. For each frequency component we get a set of M coefficients, these sets being described by certain stochastic parameters. E.g., the Fourier coefficients of the noise, a_n and b_n , and also the corresponding phase corrected coefficients a'_n and b'_n , can be regarded as independent and Gauss-distributed with vanishing mean values and variances $\sigma^2(a_n) = \sigma^2(b_n) = \sigma^2(a'_n) = \sigma^2(b'_n)$. For an absorption peak the variation coefficient, which is defined as the ratio of the standard deviation and the mean value, is thus $\sigma(a_n)/a_s$ (a_s = maximum coefficient of the signal, at peak position). When the sums $a^2 + b^2$, which constitute the power spectrum, are calculated for a noisy peak, this ratio amounts to

$$2 \cdot \sigma(a_n)/a_s :$$

$$a = a_{\text{signal}} + a_{\text{noise}} = a_s + a_n ,$$

$$b = b_{\text{noise}} = b_n \text{ (as } b_s = 0) ,$$

$$a^2 + b^2 = a_s^2 + 2 \cdot a_s \cdot a_n + (a_n^2 + b_n^2) , \quad (9)$$

where the term in brackets is negligible. $\sigma(a^2 + b^2)$ and $\mu(a^2 + b^2)$ (μ denotes the mean value) are then given by

$$\sigma(a^2 + b^2) = \sigma(a_n) \cdot a_s \cdot 2 , \quad (10)$$

$$\mu(a^2 + b^2) = a_s^2 , \quad (11)$$

$$\frac{\sigma}{\mu}(a^2 + b^2) = 2 \cdot \sigma(a_n)/a_s . \quad (12)$$

The net effect of calculating the power spectrum is thus to halve the signal-to-noise ratio in comparison with the absorption spectrum, whereas the phase correction leaves this ratio unaltered.

Experiments

We tested the technique of ten hyperfine multiplets in the rotational spectrum of pyridine-N-oxide, $\text{C}_5\text{H}_5\text{N}-\text{O}$ [4] (an example of the measurements is given in Fig. 2) and compared the resulting peak frequencies with those obtained from the power spectra and the frequencies from least-squares-fits [2] to the time domain signals (see Table 1). As far as can be

Table 1. Observed and calculated hyperfine splittings (kHz) of pyridine-N-oxide. F quantum numbers refer to upper states, in all cases $\Delta F = \Delta J$. $|v_{\text{calc.}}|$ = calculated splittings, other columns: deviations.

$J', K_-, K_+ \rightarrow J'', K_-, K_+$	$F-F$	$ v_{\text{calc.}} $	v_{fit}	v_{abs}	v_{pow}
4 3 2 \rightarrow 3 3 1	5-3	100	-3	-2	+16
	5-4	266	+1	+1	-17
5 2 3 \rightarrow 4 2 2	6/4-5	84	-2	-1	+15
	6-4	36	-4	+1	+16
5 3 2 \rightarrow 4 3 1	6-5	162	+3	+1	-7
	6-4	71	-3	0	+18
5 4 1 \rightarrow 4 4 0	6-5	244	+1	-1	-7
6 2 5 \rightarrow 6 0 6	7/5-6	96	0	+3	+26
7 2 6 \rightarrow 7 0 7	8/6-7	112	0	+2	+9
	8-6	27	0	-11	+4
7 1 6 \rightarrow 7 1 7	8-7	188	+1	+4	-11
	8-6	31	+3	-1	+4
7 2 5 \rightarrow 7 2 6	8-7	218	0	+2	0
12 4 8 \rightarrow 12 4 9	13/11-12	164	-3	-2	+2
19 6 13 \rightarrow 19 6 14	20/18-19	147	+1	+4	+6

judged from the variances σ^2 of the analyses of the hyperfine splittings, the phase corrected absorption spectra are nearly as useful as the least-squares-fit, and far better than the power spectra ($\sigma_{\text{abs}} = 3.5$ kHz, $\sigma_{\text{fit}} = 2.1$ kHz, $\sigma_{\text{power}} = 13$ kHz).

Another disadvantage of power spectra, the possible hiding of lines with both left and right neighbours, is completely overcome, as demonstrated in Figure 3. This figure shows a 3 MHz-section of the rotational spectrum of 2-fluoroacetamide, containing the $J, K_-, K_+ = 2, 0, 2-1, 0, 1$ transition split by nuclear quadrupole coupling. The dashed and dotted traces are the positive and negative root of the power spectrum (i.e., the amplitude spectrum), respectively, and the solid curve is the phase corrected absorption spectrum. The hyperfine component $F = 2-1$ is clearly revealed only by the latter. This property of the phase corrected absorption spectra is probably the most important.

Acknowledgements

We thank the members of our group for fruitful discussions. Funds provided by the Land Schleswig-Holstein, the Fonds der Chemie, and the Deutsche Forschungsgemeinschaft are gratefully acknowledged. We would also like to thank Prof. Dr. M. C. L. Gerry, Vancouver, for critically reading the manuscript.

- [1] I. Merke and H. Dreizler, *Z. Naturforsch.* **43a**, 196 (1988).
- [2] J. Haekel and H. Mäder, *Z. Naturforsch.* **43a**, 203 (1988).
- [3] D. Ziessow, On-line-Rechner in der Chemie, de Gruyter, Berlin 1973, S. 300 ff.

- [4] N. Heineking and H. Dreizler, 10th Colloquium on High Resolution Molecular Spectroscopy, Dijon 1987, Poster L19.